Modelling the Structural Dynamics of Electrical Overhead Line Power Conductors

Mohammed A. AlAqil[1*], Konstantinos Kopsidas[2]

[1, 2] Department of Electrical and Electronic Engineering, The University of Manchester, Manchester, UK
*mohammedabdulaziz.alaqil@manchester.ac.uk

Abstract – The physical phenomenon considered in this paper is Aeolian conductor vibration, which implicates the flow of air across high-voltage Overhead Line (OHL) conductors where the Aerodynamic Forces are induced through the vortex-shedding on the conductor's wake. To model this phenomenon, the structural dynamics of the Fluid-Structure Interaction (FSI) are reviewed, in the case of OHLs, to compute the Aerodynamic Forces acting on the OHL conductor. The best application found to assist in building this model is the Fluid-Structure Interaction example found in COMSOL built-in applications library. On a different study, the OHL conductor's geometry is created in COSMOL to perform the vibrations fatigue analysis and therefore determine the importance of considering the layer-to-layer interaction. The vibrations fatigue model requires the use of Structural Mechanics physics of the 3-D model by making use of the Beam and Solid Mechanics interfaces found in the Vibration Analysis of a Deep Beam example which is found in the application library. This analysis relies heavily on the accuracy of the used identity/contact pairs and material properties. The simulation results are corroborated with the reported experimental data.

Keywords: Aeolian vibration, COMSOL, power conductors, FEM, overhead lines, stranding shape

1. Introduction

As a general definition, the presence of any repeated motion after a regular interval of time is known as vibrations. The basic theory of vibrations is described by the system of forces acting on a moveable and deformable body. The natural phenomena existing in the universe such as earthquakes, water waves (i.e., tidal), sound or noise (i.e., Aeolian tone), and light are the result of transmitted waves that are described by propagating vibrations in space. The characteristics of vibrations are usually quantified by measuring the resultant vibration wave amplitude, frequency, velocity, and wavelength. Moreover, the medium of vibration has a significant impact on the mechanism of the structural vibration motion, which depends on the fluid properties and impacted structure geometry.

One of the main assets in electrical power systems is Overhead Lines (OHLs), which are placed outdoors and exposed to various environmental conditions. The most common OHLs wind-induced structural motion is Aeolian conductor vibrations. The solid beam theory is merely implemented to model OHL conductors to predict their vibration response, based on the assumption of homogenized properties. To further improve this theory, two models are considered in this paper to examine the effect of the complex conductor geometry:

1. Computing wind-conductor interaction (i.e., Aerodynamic Forces).
2. Predicting the cyclic vibration fatigue stresses for the real conductor design.

Computational Fluid Dynamics (CFD) and Structural Mechanics associated with existing COMSOL numerical capabilities are a powerful tool for this study. Hence, they are used to solve the Fluid-Structure Interactions (FSI) and the effect of the cyclic bending response on the OHL conductor real geometry.

2. Theoretical Background – Wind-Induced Motions on Overhead Line Conductors

OHLs are constructed outdoors in different environmental conditions and terrains, which make them susceptible to various types of wind-induced motions that are experienced mostly by the power conductors. Mechanical vibrations constitute a significant distraction and may harm OHL conductors through fretting fatigue [1]. In general, wind-induced conductor motions are categorised into three forms: (i) Aeolian conductor vibrations, (ii) conductor galloping, and (iii) wake-induced oscillations. Aeolian conductor vibrations are the most commonly reported type that contribute to the long-term damage of the power conductor wires and its fittings [2, 3].

Most of the experimentations associated with Aeolian conductor vibrations are performed in costly indoor/outdoor test-spans, which requires site access. The capabilities of advanced computer modelling techniques such those provided in COMSOL are deemed to be a compelling alternative tool to replicate the practical experimentations. The advanced numerical methods would be worthwhile to identify the potential risks of vibrations on OHL conductors and to overcome some of the limitations in the standard calculations.

The physical motions of OHL conductors are associated with the interaction of fluid dynamics, conductor dynamics, and efficiency of the vibrations damping system. Theoretically, the conductor's Aeolian vibratory motion is described by a set of non-linear algebraic mathematical equations that are gathered in the so-called Energy Balance Method (EBM) [4, 5]. This method is intended to quantify the OHL conductor's vibration levels (i.e., amplitude and fatigue stresses) by re-scaling the conductor's vibration mode shapes and balancing the wind power input to the conductor's vibration damping characteristics (i.e., self-damping). The aerodynamic forces are one of the primary input parameters

in the formulation of the EBM. These forces are determined experimentally in indoor wind tunnels to evaluate the aerodynamic structural-dynamics of the OHL conductors. The existing experimental and theoretical quantification of these forces are typically carried out on the homogenised conductor geometry (i.e., assuming a smooth-surface cylinder). Therefore, such modelling neglects the shape effect of the outer and inner wires in real conductor geometry [6].

In this paper, a summary of the Aeolian conductor vibration phenomenon is presented before presenting the Finite Element Model (FEM) implemented in COMSOL to compute the aerodynamic forces for single OHL conductors. Also, the three-dimensional model of the real conductor geometry is described and implemented in the vibration fatigue study. In both studies, the conductor different stranding patterns are considered in the analysis.

2.1. Description of OHL Conductors' Dynamics Undergoing Wind-Induced Motion

The physical phenomenon (i.e., Aeolian vibration) considered in this study implicates the flow of air across high-voltage OHL conductors causing wind-induced vibratory motions. The Computational Fluid Dynamics (CFD) associated with commercially available COMSOL computation packages are alternatives to solve this complex modelling problem involving Fluid-Structure Interaction (FSI).

Wind-induced conductor motions are the result of wind splitting on the back side (leeward) of the conductor when exposed to blowing wind (Fig. 1). This aerodynamic motion of air-split generates a low-pressure region on the leeward which causes the air to move in the vacuum area initializing the formation of vortices. The vortex-shedding pattern created on the leeward of the conductor produces an imbalanced alternating pressure triggering a vertical motion of the conductor in the perpendicular plane to wind intake direction [2, 3]. The generated vortex-shedding induces aerodynamic forces known as the Lift (F_L) and Drag (F_D) forces that are developed on the OHL conductor as illustrated in Fig.1. The computation of these forces is described in the next subsection.

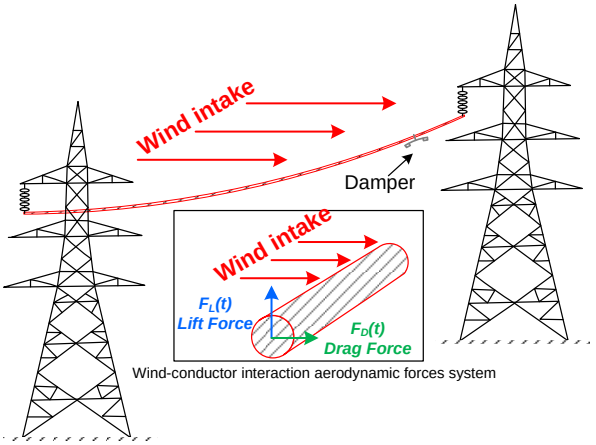

Fig. 1 Electric overhead line power conductors in the course of wind creating the aerodynamic forces

2.2. Computation of the Aerodynamic Forces

The OHL conductor undergoes a periodic cyclic aerodynamic forces where the oscillations of F_D are small compared to F_L [3, 9]. In fact, the oscillations of F_L occur at the frequency of the vortex-shedding whereas F_D oscillates at double the vortex-shedding frequency due to the alternating vortices on the conductor wake [3, 10]. The dimensionless F_L and F_D are introduced by the coefficients given by equations (1) and (2), respectively.

$$C_L = \frac{F_L(t)}{0.5 \times \rho \times V^2 \times D} \tag{1}$$

$$C_D = \frac{F_D(t)}{0.5 \times \rho \times V^2 \times D} \tag{2}$$

The variables in (1) and (2) above include the fluid stream density (ρ), velocity (V), and conductor diameter (D).

2.3. Terms used to Describe the Fluid-Structure Interaction

The vortex-shedding frequency is generated by wind when passing through the conductor in the path of flowing fluid [4]. The frequency of vortex-shedding is governed by the diameter of the conductor and velocity of the flowing fluid as expressed in Vincent Strouhal relationship shown by equation (3) [11].

$$f = S_t \frac{V}{D} \tag{3}$$

The Strouhal number (S_t) describes the mechanism of the fluid-induced oscillations and expresses the relationship between the vortex-shedding frequency (f), fluid velocity (V), and diameter (D) [6, 12].

The influence of fluid properties on the conductor dynamics is also described by another dimensionless number known as Reynolds number (Re) and expressed by (4). It defines the fluid flow conditions based on the ratio of inertial forces to the viscous property of the fluid.

$$Re = \frac{\rho V D}{\mu} \tag{4}$$

The value of Re depends on the properties of flowing fluid around the modelled geometry, which include density (ρ) and dynamic viscosity (μ) of the flowing fluid as defined in (4) [11, 13]. Both numbers (S_t and Re) are related through the empirical formula shown in (5) [6].

$$S_t = 0.198 \times \left(1 - \frac{19.7}{Re}\right) \tag{5}$$

There are three numerical techniques used to model and solve a complex system represented by partial differential equations (PDEs), namely: (i) Finite Element Modelling, (ii) Finite Difference Modelling, and (iii) Finite Volume Modelling. The main difference between these modelling techniques is the approximation of model variables and discretization techniques used. However, the work presented in this paper is mainly focused on the application of FEM.

2.4. Fatigue due to the Cyclic Bending of the Real OHL Conductor Design

There have been many experimental efforts in the industry to standardize conductor vibrations and their associated damages in the form of fatigue. There are two theories used respectively to calculate the vibration amplitude and vibration stresses which are: Energy Balance Method (EBM) and the Poffenberger-Swart theory. The Poffenberger-Swart (P-S) formula expressed in (6) is the most common practice that has been adopted by IEEE since 1960s [12-14].

$$\sigma_a = \frac{(E_{al} \times d \times T / EI)}{4(e^{(-\sqrt{T/EI}x)} - 1 + \sqrt{T/EI}x)} \times Y_b \quad (6)$$

The P-S formula calculates the maximum bending stress (σ_a) by knowing the conductor tension (T), bending stiffness (EI), and the maximum bending amplitude (Y_b) at a distance (x=89mm) from the last point of contact (LPC) on the clamp.

3. Replicating Wind-Conductor Interaction and Fatigue Stresses Calculations in COMSOL

The phenomenon of Aeolian conductor vibrations is established in COSMOL to replicate the wind tunnel practical tests. The FEM approach here involve creating the fluid domain (i.e., wind) interaction with the structural domain (i.e., OHL conductor). The FSI analysis is implemented to couple both domains from which the numerical simulations are obtained. Before computing the aerodynamic forces acting on the OHL conductors, the modelling of the fluid and conductor domains are detailed in the following subsections.

3.1. The Dimensions and Boundary Conditions of the Wind Tunnel

Fluid Domain Model: The boundary conditions and meshing of the designed conductor geometry and fluid domains have a significant influence on the accuracy of the simulation results. Therefore, the accuracy and time consumed by the simulations are critical constraints in the proposed FEM model. To improve the accuracy of the model, the meshing size and boundary conditions effect should be minimised by setting the appropriate dimensions. A balance between reducing the simulation time and achieving accurate results should be carefully considered. An Extremely Coarse mesh might produce erroneous results while an Extremely Fine one requires powerful computing resources and longer time.

Taking the abovementioned considerations into account, the fluid domain is created in COMSOL with its dimensions being carefully specified. After extensive modelling attempts, the optimum dimensions of the fluid domain boundaries have been identified in Fig.2. The dimensions are determined in terms of conductor diameter (D). The height is specified as 10D for the wind inlet and outlet, the downstream length is 5D, the upstream length is 45D, and the total length is 50D. Two symmetric boundaries bound the model, indicated as wall #1 and wall #2. Both walls bound the fluid domain with the height of the wind tunnel being selected to avoid the effect of boundary conditions on the simulation results.

Conductor Domain Model: The structured domain in COMSOL represents the geometry of the OHL conductor in the model. The design of the conductor geometry includes modelling the outer and inner layers. However, this study uses a simplified modelling assumption which considers the outer stranding shape of the conductor while assuming homogenized internal layers.

The two most common OHL conductor stranding shapes are round-stranded (RW) and trapezoidal-stranded (TW) designs. The conductors have been modelled in COMSOL based on the structures seen in Fig.2. The initial study considers the homogenized conductor structure (Fig.2), which is modelled as a solid cylinder with a smooth-surface. The RW and TW stranding shapes in Fig.2 are designed utilizing Computer Aided Design software (CAD) and imported to the COMSOL model. This study uses SOLIDWORKS software for building the conductor CAD designs. The conductor has a strand diameter (d) with a number of strands (η) in the outer layer.

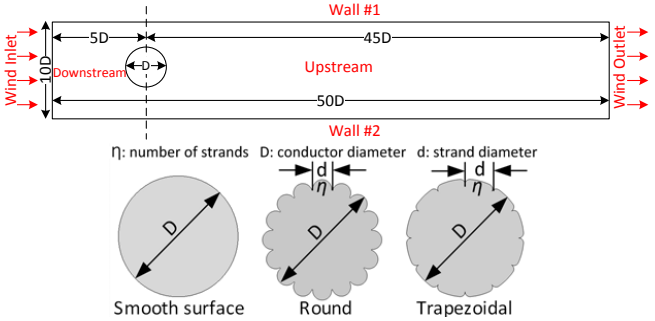

Fig. 2 Wind tunnel design and cross-section of conductor models

The wind flow around the conductor is modelled based on Fig.2 to compute the aerodynamic forces. The model simulates the wind flow around a stationary conductor in COMSOL by solving the Navier-Stokes equation, shown in (7), to compute the F_L and F_D forces. Both forces are computed by integration of pressure, inertial, and viscous forces within the boundaries of fluid and conductor domains. The variables in (7) include fluid pressure (p_f), applied external forces on the fluid field (F_f), fluid velocity (u), fluid pressure (p), time (t), and identity tensor (I).

$$\underbrace{\rho\left(\frac{\partial V}{\partial t} + u \cdot \nabla u\right)}_{\text{Inertial Forces}} = \underbrace{-\nabla p_f}_{\text{Pressure Forces}} + \underbrace{\nabla \cdot (V(\nabla V + (\nabla V)^T) - \frac{2}{3}\mu(\nabla \cdot V)\mathrm{I}) + F_f}_{\text{Viscous Forces}} \quad \underbrace{\qquad}_{\text{External Applied Forces}} \quad (7)$$

3.2. Computed Aerodynamic Forces Around Power Conductors

The proposed FEM model is initially executed to compute the aerodynamic forces acting on the conductor for the different conductor stranding shapes and sizes as illustrated in Fig.2 above. The sensitivity of the model to the generated mesh elements size is also examined. Furthermore, the effect of conductor outer shape is carried out. Finally, the simulation results are extracted and compared against experimental data.

The FEM model is implemented on a Drake size conductor that has a 28.11mm diameter and exposed to a

laminar wind flow at a speed of 0.103m/s (i.e., Re = 200) and temperature of 20°C. The standard air material properties are considered assuming a density and viscosity of 1.225 kg/m^3 and 1.78×10^{-5} kg/m·s, respectively.

The mechanism of Aeolian vibration is well captured in COMSOL as shown in Fig.3. The wind flowing across the conductor creates a vacuum area forcing the high-pressure air to move towards it and initiate the vortex-shedding as seen in the steps of Fig.3. The vortices created on the wake of the conductor are shed in an alternating fashion exerting the periodic transversal and longitudinal forces (i.e., F_L and F_D). These wind-induced forces define the Aeolian vibrations phenomenon on OHL conductors. The vortex-shedding around a stationary Drake size conductor with a smooth cylindrical surface is qualitatively obtained as seen in the upstream of Fig.3.

The computed lift (C_L) and drag (C_D) coefficients are plotted against the time history in Fig. 4 (left). The C_L and C_D alternating periodic cycle limits are provided in the form of a Lissajou diagram as shown in Fig. 4 (right). It can be seen in the C_L–C_D cycle limit diagram that F_L and F_D alternate periodically with two drag cycles occurring at one cycle of the lift. The results shown in Fig. 4 are in good agreement with the experimental data reported in [14].

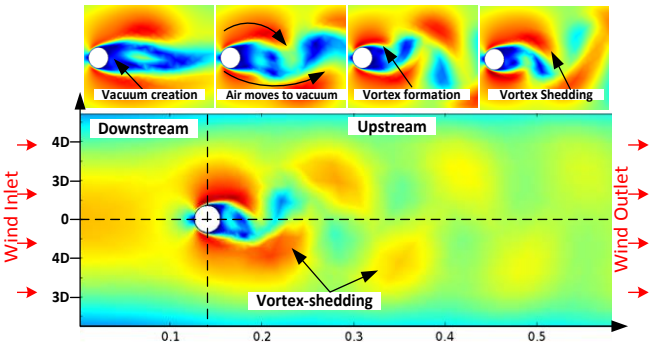

Fig. 3 Formation of the vortex-shedding around a single conductor

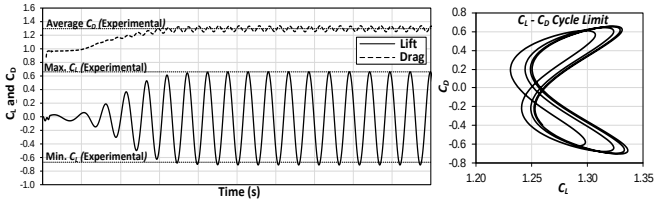

Fig. 4 Computed aerodynamic forces in COMSOL for Drake ACSR

It is evident from Fig. 4 that C_L average value is close to zero and the average F_D is 1.32 which is in good agreement with the experimental data obtained for cylinders with similar Re. Moreover, the Finite Fourier Transformation (FFT) study is used in COMSOL to obtain the frequency of vortex-shedding and found to be 0.6325 Hz. Therefore, the calculated S_t (from (2)) is almost 0.18 which is very close to the S_t for the same R_e found in [23].

The meshing of the model elements is a critical factor in modelling the wind-conductor interaction and computing the aerodynamic forces. To evaluate the sensitivity of the model to the mesh size, the following three sizes were generated: (i) Coarse mesh, (ii) Fine mesh, and (iii) Extremely Fine mesh as illustrated in Fig.5. It is noticed that the interaction layer on the surface of the conductor has narrower and smaller meshed elements which significantly influence the computation time. The sensitivity of the computed aerodynamic forces to the three mesh sizes have been investigated for a smooth-surface cylinder as demonstrated in Fig. 8. It is evident from Fig. 8 that the Extremely Fine mesh provides accurate outputs as compared to the experimental data.

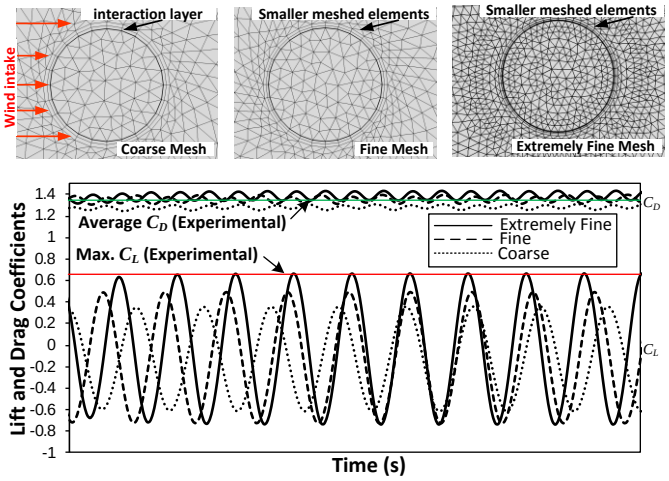

Fig. 5 Sensitivity of meshing type on the Aerodynamic forces simulations

The aerodynamic forces are computed for stranded conductors of different sizes and compared against the smooth cylinder. The number of strands and diameter of the conductor outer layer change with its size. The computations are performed at a fixed wind speed of 1 m/s. Fig.6 summarizes the variation of C_D and C_L for two sizes of smooth-cylinder and RW and TW stranded conductors.

It is evident from Fig.6 that C_D and C_L increase with the increase in conductor diameter. In fact, the RW stranding shape of a given conductor size has the highest C_D. The TW stranded conductors have better aerodynamic performance compared to RW designs of the same conductor size due to its compact design and less resistance to the wind flow. The more the number of strands on the outer layer, the less the predicted aerodynamic forces. Therefore, a higher number of strands results in better aerodynamic performance. The discrepancy of the results might also be attributed to the heating effect of the outer geometry surface.

The results show that the stranding shape has a considerable influence on the aerodynamic forces experienced by the conductor as seen in Fig. 10. Therefore, it is expected that the stranding design will also influence modelling wind power input. The forces obtained for RW conductors are the highest. On the contrary, TW conductors experience less force compared to RW conductors. This is due to the compact structure of strands in the trapezoidal designs. It is also worth mentioning that difference error is more significant at high R_e.

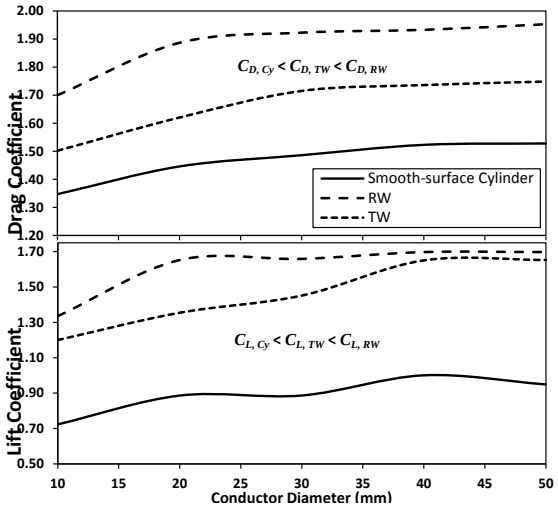

Fig. 6 Lift and drag coefficients for different conductor sizes at laminar wind speed of 1 m/s

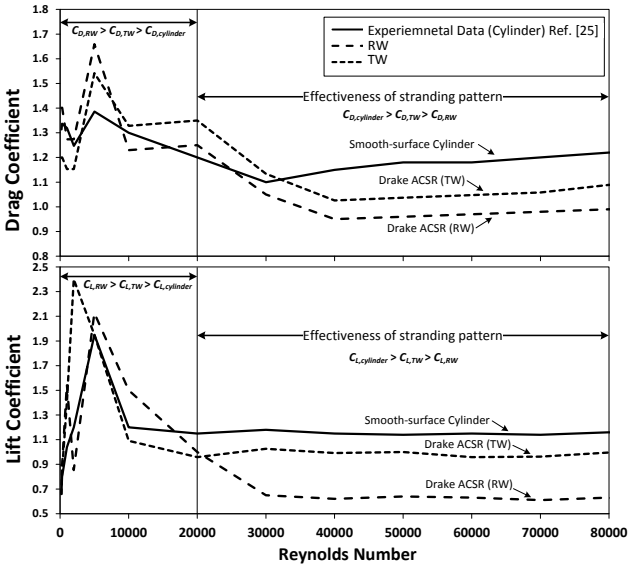

Fig. 7 Lift and drag coefficients for the three geometries

The presented FEM approach is executed to examine the impact the conductor outer stranding shape on the computations of F_L and F_D. The flow of wind around the RW and TW type conductors has been modelled as seen in Fig. 2 above. The results are demonstrated in Fig.8 below and compared against the experimental data reported in [25].

Although the smooth cylinder has a better drag for low *Re* numbers, the outer strands shape has a significant influence on dropping the drag of the conductor at high *Re* numbers. The highest drag coefficients are 1.4 and 1.56 for the smooth-surface and TW, respectively. The RW stranded conductor has the highest C_D which is 1.68. The same is observed for the C_L of the three models as compared in Figure 6. The effectiveness of the stranding shape is prominent on the response of the RW and TW as those allow gradual flow separation compared to the smooth-surface cylinder. The RW stranding shape reduces the C_L from 2.1 in the smooth cylinder to 1, which can significantly lower the amplitudes of Aeolian vibration and, as a result, minimizes the associated fatigue risk.

The flow around smooth and non-round geometries tend to become stable at a certain Reynolds number as indicated in Fig.7. It is observed that at higher Reynolds numbers (higher wind speeds) flow on the conductor leeward becomes asymmetric, which means more turbulent in nature. Therefore, the air flow is narrower reducing the drag force. Adding to these observations the stranding shape, it is found that aerodynamic forces oscillations are always higher for smooth geometries. It is important to carefully consider the fluid domain numerical modelling for high Reynolds numbers when modelling stranded conductors.

It is evident from the analysis above that the stranding shape and size of the outer conductor layer have a significant impact on the predictions of the aerodynamic forces. As a result, the Aeolian vibrations calculation methods should also consider this difference in the formulation of the EBM. It may also be necessary to consider the inner stranding pattern.

3.3. Predicted Fatigue Stresses for the Real Design of the Power Conductors

The advanced computer modelling in COMSOL is utilized to assess the cyclic Aeolian vibration that is exhibited as a forced bending amplitude on the boundary of the extruded conductor geometry (see Fig.8). Before executing the model, the conductor design is developed based on its mechanical and material properties by laying the aluminium layers around the steel core (see Fig.8). The fatigue stress is measured at 89 mm from the Last Point of Contact (LPC) with clamp after completing one bending cycle.

The boundaries at both ends (in Fig. 2) are fully coupled and consider the free and constrained strands movement. The fixed boundary end constrains all moments (M) and angles of rotation (ϕ) degrees of freedom (DoF) in all directions. The free end undergoes a tensile force and one complete bending cycle with DOFs constrained except for the horizontal axis.

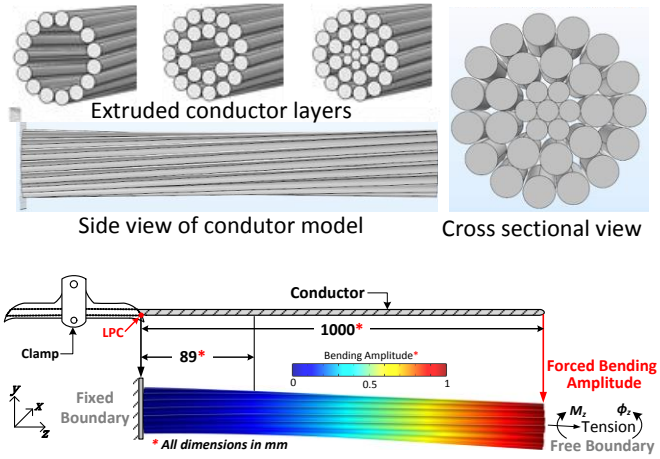

Fig. 8 Extruded conductor model and boundary conditions for conductor vibration fatigue analysis

The simulations show a nonlinear bending behavior for conductors with more than one layer. This is prominent from the simulations shown in Fig.9. It is observed that the fatigue stresses are less for the TW design compared to the RW

design as seen in Fig. 9. The FEM simulations show that RW strands experience higher fatigue stresses due to the smaller contact surface areas between its overcrossing layers compared to the TW design. Unlike the elliptical contact areas between RW strands, TW strands form a wider rectangular area, as illustrated in Fig. 9.

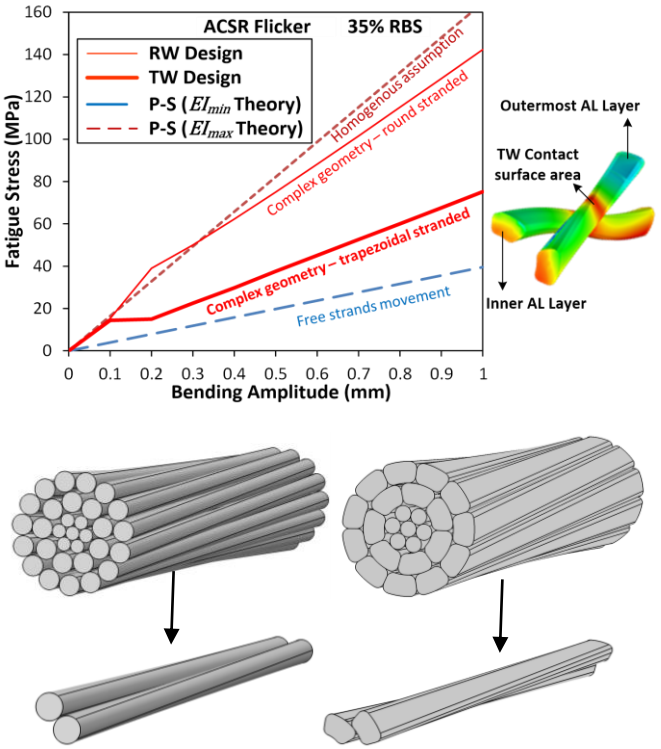

Fig. 9 Round stranded (bottom-left) Vs. Trapezoidal ACSR (bottom-right) Conductors with cross contact surfaces

4. Conclusion

In this study, a FEM model has been developed to quantify Aeolian vibrations. The model has been limited to computing the aerodynamic forces. The FEM simulations are verified with wind tunnel experimental data. The results show that aerodynamic forces predictions corroborated with the FEM model. The aerodynamic forces have also been calculated for different conductor sizes and stranding shapes using the same model. It has been shown that the outermost layer stranding shape alone has an impact on the predicted aerodynamic forces. In fact, the fatigue model included the conductor inter-layer interactions are captured and the conductor complex geometries (e.g., trapezoidal or round strands) can be assessed. This modelling attempt indicates the importance of modelling the conductor complex geometry when modelling Aeolian vibrations.

5. References

[1] Boniardi, M., Cincera, S., D'Errico, F., et al.: 'Fretting Fatigue Phenomena on an All Aluminium Alloy Conductor', Key Engineering Materials, 2007, pp 5-8

[2] Staubli, T.: 'Calculation of the Vibration of an Elastically Mounted Cylinder Using Experimental Data from Forced Oscillation', Journal of Fluids Engineering, 1983, 105, pp 225-229

[3] Diana, G., Falco, M.: 'On the forces transmitted to a vibrating cylinder by a blowing fluid', Meccanica, 1971, 6, pp 9-22

[4] Kiessling, F., Nefzger, P., Nolasco, J., et al.: 'Overhead Power Lines: Planning, Design, Construction' (Springer Berlin Heidelberg, 2003, 3rd edn., 2014), pp 321-338

[5] CIGRE: 'Modelling of Aeolian Vibration of Single Conductor: Assessment of the Technology', 1998.

[6] Kraus, M., Hagedorn, P.: 'Aeolian vibrations: wind energy input evaluated from measurements on an energized transmission line', IEEE Transactions on Power Delivery, 1991, 6, pp 1264-1270

[7] Vecchiarelli, J.: 'Aeolian vibration of a conductor with a Stockbridge-type damper'. PhD Thesis, University of Toronto, 1997

[8] Rawlins, C.: 'The long span problem in the analysis of conductor vibration damping', IEEE Transactions on Power Delivery, 2000, 15, pp 770-776

[9] Hurlbut, S., Spaulding, M., White, F., 'Numerical Solution for Laminar Two Dimensional Flow About a Cylinder Oscillating in a Uniform Stream', Journal of Fluids Engineering, 1982, 104, pp 214-220

[10] Meynen, S., Verma, H., Hagedorn, P., et al.: 'On the numerical simulation of vortex-induced vibrations of oscillating conductors', Journal of Fluids and Structures, 2005, 21, pp 41-48

[11] EPRI: 'Transmission Line Reference Book: Wind-Induced Conductor Motion (Orange Book)', 2006

[12] Van Dyke, P., Havard, D., Laneville, A.: 'Effect of Ice and Snow on the Dynamics of Transmission Line Conductors', in Farzaneh, M. (Ed.): 'Atmospheric Icing of Power Networks' (Springer, 2008), pp 171-228

[13] Papailiou, K. O.: 'Overhead Lines', (Springer International Publishing, 2016, 1st edn.), pp 559-602

[14] Blevins, R. D.: 'Flow-induced vibration', (Van Nostrand Reinhold, 1990)

[15] Feng, C.: 'The measurement of Vortex-induced effects in Flow Past Stationary and Oscillating Circular and D-section cylinders'. MSc Thesis, University of British Columbia, 1968

[16] Barry, O.: 'Finite element analysis of a single conductor with a Stockbridge damper under Aeolian vibration'. MSc Thesis, Ryerson University, 2010

[17] Oliveira, A., Freire, D.: 'Dynamical modelling and analysis of aeolian vibrations of single conductors', 1994, IEEE Transactions on Power Delivery, 9, pp 1685-1693

[18] CIGRE: 'Modeling of Aeolian Vibrations of a Single Conductor Plus Damper: Assessment of Technology', 2005

[19] Barry, O., Zhu, Y., Zu, J., et al.: 'Free Vibration Analysis of a Beam Under Axial Load Carrying a Mass-Spring-Mass', 2012, pp. 791-796

[20] Hassanpour, P., Esmailzadeh, E., Cleghorn, W., et al.: 'Generalized Orthogonality Condition for Beams with Intermediate Lumped Masses Subjected to Axial Force', 2010, Journal of Vibration and Control, 16, pp 665-683

[21] Kirk, C., Wiedemann, S.: 'Natural Frequencies and Mode Shapes of a Free–Free Beam with Large End Masses', 2002, Journal of Sound and Vibration, 254, pp 939-949

[22] Chang, T., P., Chang, C., Y.: 'Vibration Analysis of Beams with a Two Degree-of-Freedom Spring-Mass System', International Journal of Solids and Structures, 35, pp 383-401

[23] Braga, G., Nakamura, R., Furtado T.: 'Aeolian Vibration of Overhead Transmission Line Cables: Endurance Limits', IEEE-PES Transmission and Distribution Conference and Exposition: Latin America, 2004, pp 487-492

[24] Rajani, B., Kandasamy, A., Majumdar S.: 'Numerical Simulation of Laminar Flow Past a Circular Cylinder', Applied Mathematical Modelling, 2009, 33, pp 1228-1247

[25] Qi, L., Wang, M., Xu, G., et al.: 'Numerical Simulation of Aerodynamic Forces of ACSR Conductor', the International Conference on Applied Science and Engineering Innovation, Jinan, China, 2015